doi: 10.15407/ujpe62.10.0874

N.V. BONDAR,[1] M.S. BRODYN,[1] N.A. MATVEEVSKA,[2] T. BEYNIK[2]

[1] Institute of Physics, Nat. Acad. of Sci. of Ukraine
(46, Prosp. Nauky, Kyiv 03028, Ukraine; e-mail: jbond@iop.kiev.ua)
[2] Institute for Single Crystals, Nat. Acad. of Sci. of Ukraine
(60, Prosp. Nauky, Kharkiv 61001, Ukraine)

PERCOLATION THRESHOLD AND LUMINESCENCE IN FILMS OF BINARY MIXTURES OF SPHERICAL PARTICLES COVERED WITH QUANTUM DOTS

PACS 73.21.La, 78.55.Ft

The results of experimental studies of films fabricated on the basis of binary mixtures consisting of bare submicron silica particles (SPs) and silica particles covered with CdS quantum dots (NPs) are reported. The performed analysis concerns various coverage degrees and various SP-to-NP concentration ratios. By analyzing the sedimentation time and the absorption and luminescence spectra of the NP and SP aqueous suspensions and their mixtures, two exciton percolation thresholds are revealed: quasi-two-dimensional (2D) and bulk (3D) ones. The former arises in an ensemble of CdS quantum dots on the SiO_2 surface at a critical coverage value, when the wave function of excitons spans over the whole surface of NPs. The latter occurs in the binary-film plane at the critical concentration of NPs in the binary mixture. The phase transition is found to take place only if the system is above the both thresholds, which is confirmed by the optical spectra of the specimens.

K e y w o r d s: quantum dots, films, luminescence.

1. Introduction

An important feature of the percolation transition in a two-phase system is a drastic variation of a certain parameter of this system (electric or heat conductivity, transport coefficients, elasticity, and others), which occurs at the critical concentration of either of the phases. For example, in a dielectric matrix (glass or polymer) with metal inclusions or in the mixtures of conducting and nonconducting particles, the conductivity drastically increases at the critical magnitude of the conducting phase concentration [1, 2]. The origin of this phenomenon consists in the emergence of a certain fractal structure, namely, an infinite percolation cluster of connected conducting particles, when their concentration in the matrix reaches the critical value.

Nowadays, the percolation cluster formation is considered to be a well studied process. It is based on the idea of a physical cluster with confined dimensions, in which every particle contacts directly with a certain number of its closest neighbors [1–14]. Two particles are considered to be connected if they contact through their surfaces or if they are linked by means of a chain of other cluster particles [1, 3, 6]. The nature of this connection is specific in each case. The most simply one can imagine a cluster of conducting particles, when an excitation of one of them expands over the whole cluster volume within a time interval that is shorter that the own lifetime.

At a low concentration of the percolation phase, its particles are mainly monomers, and only an insignifi-

cant number of them form dimers, trimers, tetramers, and so forth. With the growth of the concentration, the number of finite-size clusters increases until a threshold concentration is reached, when a percolation cluster is formed, and a percolation phase transition takes place in the system. Hence, the formation of finite-size clusters in a solid matrix in the absence of interaction between the particles is a problem of statistical physics, and the probability of this process is proportional to the number of particles constituting the percolation phase in the matrix volume [1].

For today, it is definitely established that only one percolation threshold or one threshold concentration can exist in two- and three-dimensional systems, provided no crossover [15–17]. Nevertheless, in the late 1980s, it was found that some mechanisms can give rise to the formation of two or more percolation thresholds. For instance, in the AgI or LiI ionic semiconductor with encapsulated spherical micron- and larger-sized Al_2O_3 or SiO_2 particles, the interface layers around the latter enhance the structure conductivity by two to three orders of magnitude [16,17]. The conductivity starts to drastically grow at a definite concentration of the inert phase, $p = p_{c1}$, reaches a maximum, and then decreases to the initial value at $p = p_{c2}$. This phenomenon was also detected in other mixed structures, and it was coined in the scientific literature as a system with two percolation thresholds [16, 17]. However, we suppose that the phenomenon described in works [15–17] is a two-stage percolation associated with the reconstruction of the internal structure of the specimen rather than the change of its dimensionality.

In this work, on the basis of our results (although without a proper mathematical justification), we show that there can exist two percolation thresholds in the system, but with different dimensionalities. For this purpose, we studied the optical spectra of the films fabricated on the basis of binary mixtures of colloidal particles: bare submicronic SiO_2 spheres (below, S particles, SPs) and those spheres covered with CdS quantum dots (QDs), SiO_2/CdS, (below, N particles, NPs) to various cover fractions. The SP-to-NP concentration ratios in the films were also different. The formation of finite-size clusters and the percolation cluster in the system concerned differs significantly from that in a solid system, because it depends not only on the concentration of particles in the suspension, but also on the interaction force between them (the pair potential) and the temperature, with the growth of the latter being able to destroy the cluster.

By studying the sedimentation time for pure SP and NP suspensions, as well as SP + NP mixtures, we found that the strong attraction, which was responsible for the formation of finite-size and percolation clusters, took place both between N particles and between S and N particles. At the same time, S particles demonstrated the mutual electrostatic repulsion. There are some models for the description of the percolation threshold in colloidal systems with the indicated types of interaction [5–12]. However, they consider the interaction between the particles of only identical or only different types. We found that, in the binary SP + NP films, only N particles can form a percolation cluster. Furthermore, this process is substantially affected by the interaction between S and N particles, which results in an increase of the percolation threshold or the critical concentration, which was marked in the well-known work [13].

Another important result obtained by us concerns the discovery of two percolation thresholds – quasi-two-dimensional (2D) and bulk (3D) ones – for excitons in the examined films. Those thresholds can be distinguished well in photoluminescence (PL) and absorption spectra. It was found that there is no crossover between those thresholds, and the exciton percolation in a film arises, when the system is simultaneously above the both thresholds. We hope for that the results obtained in this work are enough to confirm the model of two thresholds with different dimensionalities in disordered porous binary films. They can also be useful when studying the hydration of water molecules or nanoparticles on spherical surfaces of proteins and in various biological media.

2. Experimental Part

A procedure to fabricate CdS QDs with the radius $R_0 \approx 2$ nm, bare SiO_2 spheres with $R \approx 150$ nm, and SiO_2 spheres covered with CdS QDs (SiO_2/CdS) with the total radius $R_1 = R + R_0$ in aqueous suspensions was described by us earlier in works [18–20]. The cover fraction θ of the SiO_2 sphere surface with CdS QDs amounted to $\theta \approx 0.15$ or 0.5. The number of QDs was determined by scanning the spherical surface; then the QDs were directly counted making use of the AutoCAD software. The determination of the

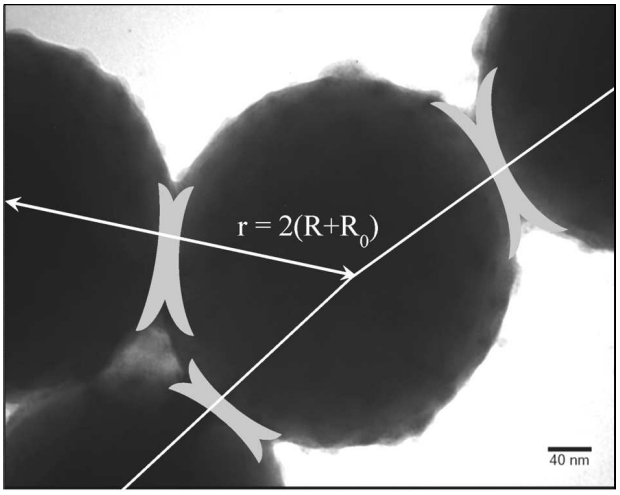

Fig. 1. TEM image of a cluster of N particles (tetramer) with CdS QDs on the surface of SiO_2 spheres. Contact areas between neighbor N particles are shown in the form of spherical caps. A distance between the centers of neighbor N particles is also indicated

θ value is a rather nontrivial task, if one takes the spherical geometry of the substrate and the QDs into account, as well as the concept of excluded volume (in the next section, this concept is described in more details). The size distributions of SPs, NPs, and QDs are determined with the help of dynamic light scattering on a Brookhaven Zetasizer NANO 5S and using a transmission electron microscope (TEM). The obtained NP ($R \approx 165$ nm) and QD ($R_0 \approx 2.4$ nm) sizes, as well as their dispersion (about 10%), testify to a rather narrow distribution of the particles and quantum dots over their dimensions and a high quality of fabricated particles. The obtained values were corrected making allowance for the corresponding hydrodynamic SP and QD diameters, which is important in the case of dynamic light scattering. This was also confirmed by the TEM data: $R \approx 150$ nm and $R_0 \approx 2.2$ nm. Figure 1 demonstrates the surfaces of N particles (with CdS QDs) associated into a tetramer cluster.

The technology of film preparation on the basis of SP + NP binary mixtures was also described in works [18–20]. Films with the thickness $d = 6 \pm 1$ μm and the concentration ratios $n_1(\text{SPs}) : n_2(\text{NPs}) = 0.8 : 0.2$, $0.6 : 0.4$, $0.5 : 0.5$, $0.4 : 0.6$, and $0.2 : 0.8$ (below, films F1 to F5, respectively), were produced on quartz substrates intended for recording the PL and absorption spectra. The parameters n_1 (for SPs) and n_2 (for NPs) can be determined in terms of the volume fractions $P_{\text{NP,SP}}$ of S and N particles with respect to their total volume ($P_{\text{SP}} + P_{\text{NP}} = 1$) and the ratio between their sizes $\alpha = R/R1$. In particular, for NPs,

$$n_2 = \alpha P_{\text{NP}}/(\alpha P_{\text{NP}} + (1 - P_{\text{SP}})).$$

However, since $R \approx R_1$, i.e. $\alpha \approx 1$, we may assume that $n_1 + n_2 \approx 1$.

Unlike the case of solid matrices, the formation of particle clusters in colloidal suspensions occurs owing to the Brownian diffusion and depends not only on the particle concentration, but also, as was mentioned above, on the pair potential. Under the microgravity action, the arising clusters sink. Therefore, by determining the sedimentation time of a suspension (the complete sedimentation on the cuvette bottom), it is possible to draw some conclusions concerning the force of interaction between either S or N particles.

We studied dilute aqueous SP and NP suspensions, as well as their $1 : 1$-mixture with the dimensionless density $\phi = (4/3)\pi R^3 \rho \approx 0.0035$. The sedimentation time for the suspension of bare SPs was found to equal 6–7 days, which is a result of the particle repulsion in the medium with $pH \approx 5.2$. For the NP suspension, the time of the complete sedimentation equaled only about 2.5 days, which was rather unexpected. The coating of the surface of SiO_2 spheres with CdS QDs makes it rough and increases the friction between the surface and the suspension. As a result, the sedimentation time should have increased in comparison with that for the suspension of bare S particles. However, it was not the case. Furthermore, we found that the sedimentation of the NP suspension depends on the cover fraction θ and amounts to 4.5 days for $\theta \approx 0.15$ and 2.5 days for $\theta \approx 0.5$. The explanation of this fact is given in the next section. Owing to the interaction between S and N particles, the film structure became highly porous and was characterized by a low coordination number z, as one can see in Fig. 2.

Figure 3 illustrates PL bands registered for a film obtained from the suspension of N particles with $\theta \approx$ ≈ 0.15 and, for comparison, a PL band obtained for film F1. The difference between the shapes and the half-height widths of both bands is the first proof of the exciton delocalization in the array of CdS QDs located on the surface, which will be discussed below.

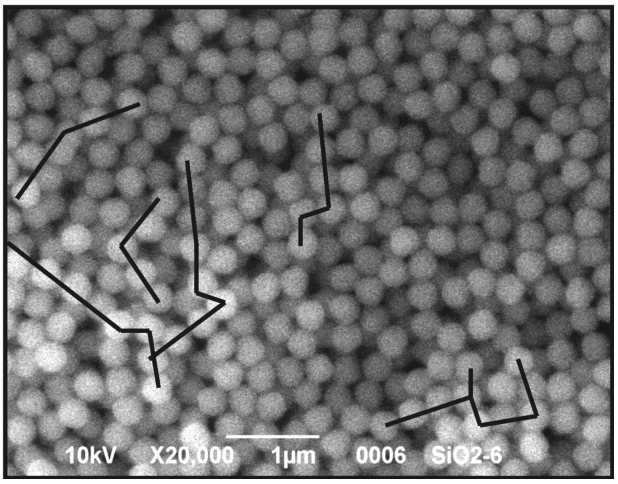

Fig. 2. TEM image of the SP + NP binary film surface. Lines mark clusters of connected N particles

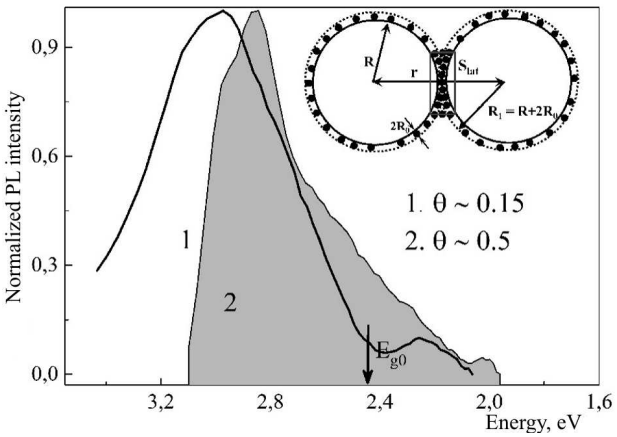

Fig. 3. PL spectra of a film of N particles with the cover fraction $\theta = 0.15$ (*1*) and film F1 (*2*). The arrow marks the energy position of the forbidden gap in CdS, $E_{g0} \approx 2.44$ eV. The inset illustrates a contact between two N particles

Figure 4 demonstrates the absorption spectra for film specimens F1 (curve *a*) and F5 (curve *b*) with the cover fraction $\theta \approx 0.5$, and for the film with bare S particles (curve *c*). Spectra *a* and *b* were obtained by subtracting spectrum *c*, which makes it evident that the PL and absorption spectra of those specimens are associated with the exciton transitions in CdS QDs located on the surface of SiO_2 spheres. Note that the absorption spectra were obtained on a spectrometer "SPEKORD M40", and the PL ones on a spectral installation with the resolution not worse than 0.5 nm. The spectra were excited using a He-Cd laser with the wavelength $\lambda_{exc} = 325$ nm and a power of about 10 MW, and measured at room temperature.

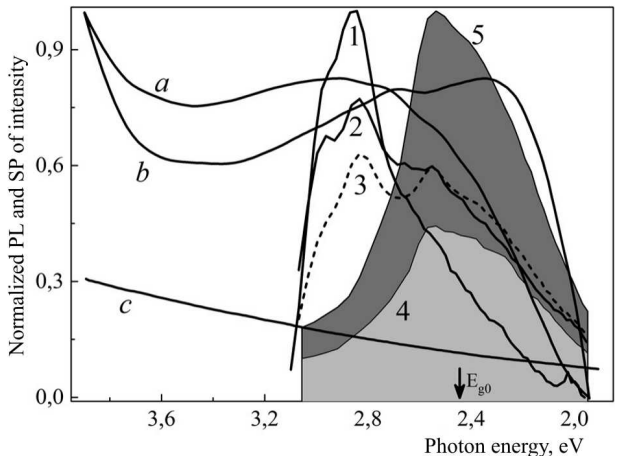

Fig. 4. Optical absorption (*a*, *b*, *c*) and PL spectra of films F1 to F5 (curves *1* to *5*, respectively)

3. Experimental Results and Their Discussion

3.1. Clustering, interaction, and surface percolation in SP + NP mixtures

Before analyzing the results obtained, let us first consider the formation of a percolation cluster of CdS QDs on a spherical surface. The surface percolation on a spherical or other convex surface is the most difficult problem, both theoretical and experimental, despite that the edge effects associated with a finite specimen size are absent. Therefore, the percolation theory does not provide an adequate way to determine the point of percolation cluster emergence in this case, unlike the 2D or 3D geometry. It is well known that the percolation of excitons results from the delocalization of their wave function over the array of QDs located on the surface, which can be classed to quasi-2D percolation. An advantage of this geometry consists in that if we know the QD concentration on a spherical surface, we can calculate the average distance between the neighbor QDs and draw conclusion about the interaction between them.

However, let us first determine the value of θ. As was already marked, this is rather a nontrivial task for the selected geometry. We consider QDs to be absolutely hard spherical particles, which are randomly deposited on the SiO_2 surface. After a QD "has

touched" the surface, it does not move, and every next QD can occupy only an empty place. The deposition process terminates, when a new QD cannot be placed on the spherical surface without its overlapping with existing QDs that were deposited earlier. Those are the main points of the random sequential adsorption (RSA) model (see work [21] and the references therein). In this case, the quantity θ can be determined as $\theta = N/N_0$, where N is the number of QDs counted on the spherical surface, and N_0 the maximum number of QDs that can be arranged on a spherical surface, using their hexagonal dense packing. The latter parameter equals [22]

$$N_0 = \frac{2\pi\sqrt{3}}{3} B^3 \left[(1 + B^{-1})^2 - 0.77\right], \tag{1}$$

where $B = R_0/R$. Unlike the expression in work [22], the brackets in Eq. (1) contain an extra term to provide the asymptotics $N_0 \to 12$ at $R_0 \to R$. Nevertheless, Eq. (1) overestimates the value of N_0, because it does not make allowance for the random character of the spherical surface coating. Therefore, we should estimate that part of the spherical surface that can be coated, θ_m. This problem can be calculated in the framework of the RSA model, which was expounded in many works.

In particular, in work [21], it was shown that the deposition of spherical particles onto a spherical surface terminates, when the so-called jamming limit is achieved. This occurs at $\theta_m = \theta_0(1 + B)^2$, where B falls within an interval of 0–0.7, and $\theta_0 \approx 0.547$ is the jamming limit for a planar surface. From whence, it follows that the surface area of SiO_2 spheres that is available for the covering with CdS QDs amounts to $S_m = 4\pi R^2\theta_m$. Then the maximum number of QDs that can be arranged in this area equals

$$N_m = S_m/\pi R_0^2 = 4\theta_0 B^{-2}(1 + B)^2,$$

and $\theta = N/N_m$. With regard for the percolation in various lattice and lattice-free models, we found that the magnitude of cover fraction, at which the probability of the exciton percolation in a QD array located on a spherical surface amounts to about 1/2 (this is the lower limit of the percolation threshold) equals $\theta \approx \theta_m/2$. Since $\theta \approx 0.5$ in our films, i.e. $\theta > \theta_m/2$, we may assert that, at this cover fraction, the excitons are delocalized in the array of CdS QDs, and the percolation threshold is exceeded.

In order to prove the aforesaid, let us consider an array of N quantum dots distributed over a spherical surface according to the Poisson law. We should calculate the quantity $\langle\xi\rangle/2R_0$, where $\langle\xi\rangle$ is the average distance between the centers of nearest-neighbor QDs. Let one of DQs be located at the sphere pole. Then, the probability $P(\sigma)$ to find the nearest QD in the polar angle interval $(\sigma, \sigma + d\sigma)$ equals [23]

$$P(\sigma) = \frac{(N-1)\sin(\sigma)\left[1 + \cos(\sigma)\right]^N}{2^{N-1}\left[1 + \cos(\sigma)\right]^2}. \tag{2}$$

From whence, the average angular distance amounts to

$$\langle\sigma\rangle = \int_0^1 \sigma P(\sigma) d\sigma. \tag{3}$$

For large N-values, $\langle\sigma\rangle \approx (\pi/N)^{1/2}$ and $\langle\xi\rangle = R\langle\sigma\rangle = R(\pi/N)^{1/2}$. If the number of QDs on sphere's surface equals $N = \theta N_m$, then, for $\theta \approx \theta_m/2$, we obtain $\langle\xi\rangle/2R_0 \approx 1$. This means that, at $\theta > \theta_m/2$, the excitons are really delocalized on the surface of N particles and exceed the percolation threshold.

In order to explain why the sedimentation times for both SP and NP suspensions and the SP + NP binary mixture are different, we have to consider the processes of particle clustering in those media. In the suspension of N particles, there is a single type of the interaction between them; and there are three interaction types in the binary mixture: SP–SP, NP–NP, and SP–NP ones. The sedimentation time quickly decreases, if particle clusters, which were formed at particle collisions due to the Brownian diffusion, rather than separate particles sink under the microgravity action. The probability of the SP cluster formation is low because of a high repulsion potential between the S particles. As a result, the corresponding sedimentation rate is also low.

On the other hand, the interaction between the N particles themselves and between the S and N particles, as can be seen from short sedimentation times, is substantial and depends on θ. Qualitatively, this fact can be explained as follows. Although the S and N particles are spherical, but the contact between them is not point-like, as one can see from Fig. 1. The distance between the centers of two contacting particles (NP–NP or SP–NP) equals $r = 2R(1 + B)$. Since $B \ll 1$, the contact area between them looks like a spherical segment (cap) with the area $S_{\rm lat} = 2\pi Rh$, where $h = 2R_0$ is the segment height (see the inset in

Fig. 3). The area of the spherical segment is chosen so that the distance between the QDs located on the segments of neighbor N particles should be equal to about $2R_0$. Two N particles interact with each other following the "cogwheel" mechanism and form a layer of QDs.

It is not difficult to evaluate the number of QDs on a spherical segment ($\approx 8\theta B$); from whence, one can see that the interaction force between neighbor N particles is proportional to θ. The efficiencies of the NP and SP+NP cluster formations are proportional to the frequency and the effective coefficient A of collisions. In the framework of the polymer flocculation model, the parameter A equals $A = \theta(1-\theta)$ [24]. Let us assume, although without a proper justification, that this model is also valid in our case. Then, at $\theta \approx 0.5$ and, $A \approx 0.25$, the probability of the NP cluster formation is maximum, and the time of the NP sedimentation is minimum. A reduction of the quantity θ down to about 0.15 diminishes both the interaction force between the particles and the cluster formation probability. As a result, the sedimentation time increases. On the other hand, if the cover fraction exceeds θ_m (a second monolayer of QDs), there arises the steric repulsion between the N particles in the suspension, and the sedimentation time becomes longer as well.

The clustering in the SP + NP mixture has its specific features. In this case, the probability of the SP cluster formation is also low, whereas that of the NP clustering is high. However, if an N particle plays the role of a cluster "nucleus" and if the first cluster shell is created by N particles (at most 12), the cluster mass will grow quickly. But if the first shell is formed by S particles, which repulse one another, the cluster mass will grow slower, and the cluster itself will be temperature-unstable, because the interaction force between S and N particles is smaller. Therefore, due to the interaction between the N and S particles in the mixture, the S particles "capture" a certain number of N particles and thus raise the percolation threshold, which was marked in the well-known work [13].

3.2. Percolation transitions in binary films and their manifestations in optical spectra

Now, let us consider the emergence of the second exciton percolation threshold in the films fabricated from SP+NP mixtures. The difference between our specimens and the similar densely packed structures of spherical particles consists in a high porosity of the former (Fig. 2). This porosity is a result of the interactions (van der Waals and electrostatic ones) between particles and makes the percolation threshold higher (n_{2c}). However, only some fraction (P_c) of N particles form the percolation cluster, whereas the others are located in finite-size clusters.

The authors of work [25] established the following relation between the particle fraction P_c and the coordination number z, i.e. the number of contacts between the selected particle and its nearest neighbors in the percolation cluster, in a vicinity of the percolation threshold and above it:

$$P_c = \left[1 - \sqrt{[2 - 0.5z]^5}\right]^{0.4}. \quad (4)$$

The simulation showed that a percolation cluster arises at $z \approx 2$. At the same time, at $z = 4$, all N particles enter the percolation cluster ($P_c = 1$). As is known, this "smearing" of the P_c-value at the threshold point is resulted from the finite sizes of researched structures.

As was already mentioned, the interaction between particles in binary mixtures gives rise to a high porosity of our films and to the formation of a chain-like structure of NP clusters, as is seen in Figs. 1 and 2. Nowadays, there is no theory describing the dependences of the porosity p and the coordination number z on the particle radius R. However, the majority of experimental results known in the literature can be well approximated by the following empirical expressions [26, 27]:

$$p(R) = k_0 + (1 - k_0)\exp(-aR^b), \quad (5)$$

$$z(R) = 1.126\exp\left[3.2(1 - p(R))\right] + 0.86\exp\left[3.5(p(R) - 1)\right], \quad (6)$$

where $k_0 \approx 0.4$ is the porosity of a free (or loose) random packing of spherical particles, the quantity $a \approx 0.36$ depends on the density ρ ($\rho \approx 2.54$ g/cm^3 for SiO_2) and the Hamaker constant H ($H \approx 8 \times \times 10^{-20}$ J for SiO_2), and $b = 0.47$. Therefore, in the case $R = 0.15$ μm, we obtain $p \approx 0.82$, $z \approx 2.1$, and $P_c \approx 0.43$.

The dependences of $z(R)$ and $P(R)$ on $p(R)$ are shown in Fig. 5. One can see that, if the film porosity diminishes, $z \to z_0 \approx 6$, a value that is characteristic of the random dense packing of spherical

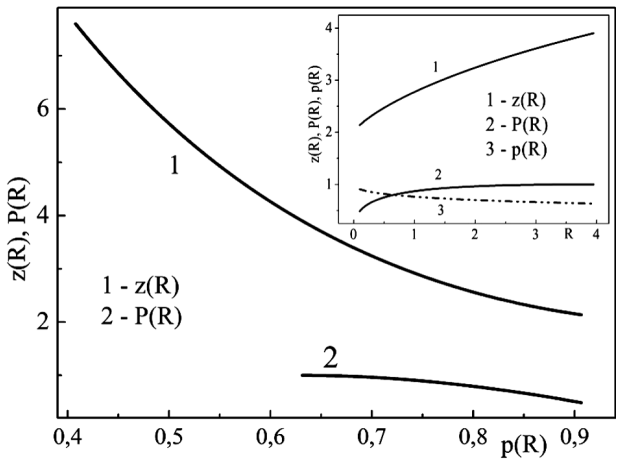

Fig. 5. Calculated dependences of $z(R)$ and $P(R)$ on $p(R)$. The dependences $z(R)$, $P(R)$, and $p(R)$ are shown in the inset

particles. The reduction of the porosity in a structure means not only an increase of the particle concentration in the film volume, but also a change of the interaction between the particles with the growth of their size (see the inset in Fig. 5). Knowing that $P_c \approx 0.43$, one can determine the number of N particles in the percolation cluster ($n_{2c^*} = P_c n_{2c}$) and their total number, which makes it possible to predict the point of the exciton phase transition in such complicated disordered structure as a binary film of spherical particles with adhesion.

However, it is rather difficult to register the moment of the phase transition of excitons in 2D or 3D arrays of semiconductor QDs, unlike, for example, the binary mixtures of conducting and nonconducting particles, in which the formation of a percolation cluster is fixed by a drastic growth of the conductance of the system. Therefore, the optical PL and absorption spectra are reliable tools to reveal the percolation of excitons in those structures.

Let us analyze the experimental proofs concerning the presence of two percolation thresholds in the examined films. The quasi-two-dimensional (2D) threshold will be considered firstly. For this purpose, let us compare the PL bands for the film formed by N particles with $\theta \approx 0.15$ and film F1 with $\theta \approx 0.5$, which are depicted in Fig. 3. The absorption spectra of those films are identical and are shown by a single curve a in Fig. 4. From our previous researches [18, 19], it is known that the delocalization of excitons in a QD array is accompanied by the disappearance of their spatial effect and a red shift of the PL band. However, now, this is not the case. The maxima of both PL bands (the main maximum in the first band and the short-wave one in the second band) are created by the annihilation of excitons in QDs. They almost coincide with each other, being shifted by about 500 meV with respect to the forbidden gap in bulk CdS ($E_{g0} \approx 2.44$ eV) due to the quantum-size effect.

In the framework of the infinitely deep potential well model and using the effective-mass method [28], let us evaluate the average radius of CdS QDs on the surface of N particles: $\langle R_0 \rangle \approx 2.1$ nm. This value agrees well with the values obtained within the TEM and dynamic light scattering methods. However, the half-height widths of those bands are strongly different. It is well known that, in a sparse array of QDs, where the excitons are localized at separate QDs, the shape of a PL band is governed by the dispersion of QDs over their size, being strongly broadened. At the exciton delocalization and the appearance of the exciton percolation, the indicated dependence on the dispersion disappears, and the PL band of excitons becomes essentially narrower. By comparing two PL bands in Fig. 3, one can see that the exciton system in specimens with $\theta \approx 0.5$ was above the percolation threshold. Nevertheless, the spatial effect survived. The latter is explained by the fact that the excitons on the surface of N particles move in a "monolayer" about $2\langle R_0 \rangle$ in thickness. Since the model of surface percolation does not provide exact methods for finding the point of percolation emergence on closed surfaces (of which a sphere is a partial case), the narrowing of the exciton radiative emission bandwidth is the most reliable tool to detect the exciton percolation in a QD array.

Now, let us consider the formation of a bulk (3D) percolation threshold in films F1 to F5. Figure 4 demonstrates the absorption spectra (curves a and b) of films F1 and F5, as well as the PL bands for films F1 to F5. The position of the PL band for films F1 with the minimum NP concentration was already discussed above. Here, we only note that its main peak is a doublet with a distance of about 120 meV between its components. A similar splitting (by about 160 meV) of the PL band for CdS QDs grown up in a glass matrix was observed in work [18, 19], in which its origin was described. This band was mainly created by monomers of N particles and by a small

number of NP clusters containing 2, 3, 4,... particles, in which the quantum-size effect for excitons disappears. It is so because the wave function of excitons in such clusters occupies their entire volume, resulting in the disappearance of the size effect. The energy of excitons $E \leq E_{g0}$ in this case, and they form the long-wave tail in the PL band (Fig. 4). A small peak in this band at about 2.0 eV arises owing to stabilizer molecules (PAA) and Si=O bonds on the SiO_2 surface. As the concentration of N particles grows (films F2 and F3), the intensity of the main peak in the PL band starts to diminish, despite that the number of QDs increases. The intensity of the second peak in the PL band at $E \approx E_{g0}$ also increases. This is a result of a larger number of NP clusters in the film. Finally, at the critical concentration of N particles $n_{c2} \approx 0.6$ (film F4), the PL band in the interval of quantum excitonic states disappears, and only the band at $E \approx E_{g0}$ testifying to the formation of a percolation cluster is observed. A further growth of the NP concentration (film F5) is accompanied by a growth of the intensity of this band, which is a result of a larger number of particles in the percolation cluster and the growth of its dimensions. This conclusion is also confirmed by the absorption spectrum b, whose maximum is shifted toward the red side (Fig. 4, film F5).

4. Conclusions

Hence, we have established that a disordered system, in particular, a binary film on the basis of spherical particles, is characterized by two percolation thresholds at corresponding critical concentrations. Those percolations have different dimensionalities, and there is no crossover between them, if the concentration of either phase increases. The main condition for the phase transition to take place is that the system must be above both thresholds simultaneously. We assert that the concept of two percolation thresholds, which is now used in the literature, describes the two-level percolation and corresponds to the reorganization in the internal structure of the specimen owing to an increase of the concentration of either of its phases; but it is not a result of the change in the specimen dimensionality.

For completeness, let us demonstrate that the interaction between particles really increases the percolation threshold [13]. For this purpose, let us consider a similar disordered structure, but without any interaction between the particles: a mixture of conducting and nonconducting macroparticles with a random dense packing characterized by the filling factor $f = 0.6$ and the porosity $1 - f = 0.4$. It is well known that the conductivity and the percolation cluster arise in this structure at the threshold concentration of the conducting phase $p_c = 0.29 \pm 0.02$, and the finite-size clusters have a compact structure [29]. In our case, the film porosity is high ($1 - f = 0.82$). Furthermore, the clusters are chain-like (Figs. 1 and 2). Therefore, their concentration in the percolation cluster has to be lower than in the previous system, and the threshold should be formed at $n_{c2} < p_c$.

But this is not the case. The first cause consists in that N particles interact not only with themselves, but also with S particles, which results in the formation of mixed clusters. The S particles in the percolation cluster are the so-called "red bonds" or blocking nodes, which prohibit the expansion of the conductivity or, as in our case, the expansion of the exciton wave function over the percolation cluster. In order to pass around such nodes, a larger number of N particles in the system is required. Second, since the deposition of QDs on a spherical surface is stochastic, they can form a percolation cluster only on one hemisphere of the N-particle surface [30]. Therefore, this particle can also be a blocking node in the percolation cluster, and the concentration of N particles in the system must be higher. Those are the main factors resulting in the "increase" of the percolation threshold in our films. The corresponding stabilization of the system will give possibility to avoid the interaction between the particles of different types and will lower the phase transition threshold. All that can find applications in biological and chemical systems, as well as in nanophysical and electronic structures.

The work was carried out in the framework of the targeted complex program of the National Academy of Sciences of Ukraine for fundamental research "Fundamental issues of new nanomaterials and nanotechnologies creation" (project NANO No. 2-16-N).

1. D. Stauffer, A. Aharony. *Introduction to Percolation Theory* (Taylor and Francis, 1992) [ISBN: 0748400273].
2. N. Johner, C. Grimaldi, I. Balberg, P. Ryser. Transport exponent in a three-dimensional continuum tunneling-percolation model. *Phys. Rev. B* **77**, 174204 (2008).
3. I. Balberg, J. Jedrzejewski, E. Savir. Electrical transport in three-dimensional ensembles of silicon quantum dots. *Phys. Rev. B* **83**, 035318 (2011).

4. I. Balberg. Electrical transport mechanisms in three-dimensional ensembles of silicon quantum dots. *J. Appl. Phys.* **110**, 061301 (2011).
5. A. Coniglio, U. De Angelis, A. Forlani, G. Lauro. Distribution of physical clusters. *J. Phys. A* **10**, 219 (1977).
6. A. Coniglio, U. De Angelis, A. Forlani. Pair connectedness and cluster size. *J. Phys A* **10**, 1123 (1977).
7. G.H. Wu, Y.C. Chiew. Selective particle clustering and percolation in binary mixtures of randomly centered spheres. *J. Chem. Phys.* **90**, 5024 (1989).
8. E. Dickinson. Simple statistical thermodynamic model of the heteroaggregation and gelation of dispersions and emulsions. *J. Colloid Interf. Sci.* **356**, 196 (2011).
9. Y.C. Chiew, E.D. Glandt. Percolation behaviour of permeable and of adhesive spheres. *J. Phys. A* **16**, 2599 (1983).
10. N. Seaton, E.D. Glandt. Aggregation and percolation in a system of adhesive spheres. *J. Chem. Phys.* **86**, 4668 (1987).
11. J. Wang, I.L. McLaughlin, M. Silber. Percolation in binary mixtures with strong attraction between unlike particles. *J. Phys.: Condens. Matter* **3**, 5603 (1991).
12. Y.C. Chiew, G. Stell, E.D. Gland. Clustering and percolation in multicomponent systems of randomly centered and permeable spheres. *J. Chem Phys.* **83**, 761 (1985).
13. A.L.R. Bug, S.A. Safran, G.S Grest, I. Webman. Do interactions raise or lower a percolation threshold? *Phys. Rev. Lett.* **55**, 1896 (1985).
14. K.S. Deepa, S.K. Nisha, P. Parameswaran, M.S. Sebastian, J. James. Effect of conductivity of filler on the percolation threshold of composites. *Appl. Phys. Lett.* **94**, 142902 (2009).
15. B. Nettelblad, E. Mårtensson, C. Önneby, U. Gäfvert, A. Gustafsson. Two percolation thresholds due to geometrical effects: experimental and simulated results. *J. Phys. D* **36**, 399 (2003).
16. H.E. Roman. A continuum percolation model for dispersed ionic conductors. *J. Phys.: Condens. Matter* **2**, 3909 (1990).
17. E. Roman, A. Bunde, W. Dieterich. Conductivity of dispersed ionic conductors: A percolation model with two critical points. *Phys. Rev. B* **34**, 3439 (1986).
18. N.V. Bondar, M.S. Brodin, N.A. Matveevskaya. Photoluminescence and exciton confinement in porous disordered films. *Fiz. Tekh. Poluprovodn.* **50**, 369 (2016) (in Russian).
19. N.V. Bondar, M.S. Brodyn. Spectroscopy of semiconductor quantum dots. *Physica E* **42**, 1549 (2010).
20. N.V. Bondar, M.S. Brodin, N.A. Matveevskaya. Quantum-size effect and exciton percolation in porous and disordered films on the basis of spherical "core/shell" elements. *Ukr. Fiz. Zh.* **60**, 649 (2015) (in Ukrainian).
21. Z. Adamczyk. *Particles at Interfaces: Interactions, Deposition, Structure* (Academic Press, 2006) [ISBN: 9780123705419].
22. M. Alonso, M. Satoh, K. Miyanami. The effect of random positioning on the packing of particles adhering to the surface of a central particle. *Powder Technol.* **62**, 35 (1990).
23. D. Scott, Ch.A. Tout. Nearest neighbour analysis of random distributions on a sphere. *Mon. Not. R. Astron. Soc.* **241**, 109 (1989).
24. R. Hogg. Collision efficiency factors for polymer flocculation. *J. Colloid Interf. Sci.* **102**, 232 (1984).
25. D. Bouvard, F.F. Lange. Relation between percolation and particle coordination in binary powder mixtures. *Acta Metal. Mater.* **39**, 3083 (1991).
26. R.M. German. Coordination number changes during powder densification. *Powder Tech.* **253**, 368 (2003).
27. C.L. Feng, A.B. Yu. Quantification of the relationship between porosity and interparticle forces for the packing of wet uniform spheres. *J. Colloid Interf. Sci.* **231**, 136 (2000).
28. *Semiconductor Nanocrystals: From Basic Principles to Applications*, edited by A.L. Efros, D.L. Lockwood, L. Tsybeskov (Springer, 2003) [ISBN: 978-1441934024].
29. K.S. Deepa, M.T. Sebastian, J. James. Effect of interparticle distance and interfacial area on the properties of insulator-conductor composites. *Appl. Phys. Lett.* **91**, 202904 (2007).
30. A. Oleinikova, N. Smolin, I. Brovchenko, A. Geiger, R. Winter. Formation of spanning water networks on protein surfaces via 2D percolation transition. *J. Phys. Chem. B* **109**, 1988 (2005).

Received 20.06.16.
Translated from Ukrainian by O.I. Voitenko

М.В. Бондар, М.С. Бродин,
Н.А. Матвеєвська, Т.Г. Бейник

ПЕРКОЛЯЦІЙНІ ПОРОГИ
ТА ЛЮМІНЕСЦЕНЦІЯ ПЛІВОК НА ОСНОВІ
БІНАРНИХ СУМІШЕЙ СФЕРИЧНИХ ЧАСТИНОК,
ПОКРИТИХ КВАНТОВИМИ ТОЧКАМИ

Р е з ю м е

У статті проаналізовані експериментальні результати дослідження плівок на основі бінарних сумішей чистих субмікронних сфер SiO_2 (SP) та вкритих квантовими точками CdS (NP) з різними величинами покриття та співвідношення концентрацій SP : NP. Дослідження часів седиментації водних суспензій SP, NP та їх сумішей, а також аналіз їх спектрів поглинання та фотолюмінесценції дозволило виявити два перколяційних порога екситонів: квазідвовимірний (2D) та об'ємний (3D). Перший виникає на поверхні NP частинок у масиві квантових точок CdS при критичній величині покриття, коли хвильова функція екситонів охоплює всю поверхню NP частинок. Другий — у площині плівок при пороговій концентрації NP частинок у бінарній суміші. Фазовий перехід виникає тільки за умови, коли система одночасно знаходиться вище обох порогів, що добре проявляється у відповідних оптичних спектрах зразків.